

NATIONAL AERONAUTICS AND SPACE ADMINISTRATION

*Technical Report No. 32-847*

*Advantages of Multipoint Control for Vibration Testing  
of Complete Ranger Spacecraft*

*Jack L. Cooper*



jpl

JET PROPULSION LABORATORY  
CALIFORNIA INSTITUTE OF TECHNOLOGY  
PASADENA, CALIFORNIA

January 1, 1966

FACILITY FORM 602

N69-76757  
(ACCESSION NUMBER)

(THRU)

NONE  
(CODE)

19  
(PAGES)

CR-105382  
(NASA CR OR TMX OR AD NUMBER)

(CATEGORY)

NATIONAL AERONAUTICS AND SPACE ADMINISTRATION

*Technical Report No. 32-847*

*Advantages of Multipoint Control for Vibration Testing  
of Complete Ranger Spacecraft*

*Jack L. Cooper*

A handwritten signature in cursive script, reading "E. L. Sheldon", positioned above a horizontal line.

E. L. Sheldon, Manager  
Environmental and Dynamic Testing Section

JET PROPULSION LABORATORY  
CALIFORNIA INSTITUTE OF TECHNOLOGY  
PASADENA, CALIFORNIA

January 1, 1966

**Copyright © 1966  
Jet Propulsion Laboratory  
California Institute of Technology  
Prepared Under Contract No. NAS 7-100  
National Aeronautics & Space Administration**

## CONTENTS

<b>I. Introduction.</b>	<b>1</b>
<b>II. Background of Multipoint Control at JPL</b>	<b>2</b>
<b>III. Equalization Techniques Using Multipoint Control</b>	<b>5</b>
<b>IV. Comparison of Multipoint Control vs Single-Point Control of Ranger Block III Spacecraft</b>	<b>9</b>
<b>V. Conclusions.</b>	<b>13</b>
<b>References</b>	<b>14</b>

## FIGURES

<b>1. Functional block diagram of the six-channel multipoint control system</b>	<b>3</b>
<b>2. Ranger spacecraft Z-axis vibration test fixture</b>	<b>4</b>
<b>3. Single-point control equalization requirement and servo-controlled acceleration curves</b>	<b>4</b>
<b>4. Multipoint control equalization requirement and servo-controlled acceleration curves</b>	<b>4</b>
<b>5. JPL six-channel control system</b>	<b>5</b>
<b>6. Functional block diagram for determining equalization requirement curve</b>	<b>6</b>
<b>7. Equalization requirement curve</b>	<b>6</b>
<b>8. Functional block diagram for verifying equalization and/or testing</b>	<b>7</b>
<b>9. Equalization verification curve</b>	<b>8</b>
<b>10. Test specification power spectral density</b>	<b>9</b>
<b>11. Ranger spacecraft, Z-axis test setup</b>	<b>9</b>
<b>12. Average PSD, multipoint control</b>	<b>10</b>
<b>13. Average PSD, single-point control</b>	<b>10</b>
<b>14. Spectra ratio, multipoint average ratioed to specification</b>	<b>10</b>
<b>15. Spectra ratio, single-point average ratioed to specification</b>	<b>10</b>
<b>16. PSD Foot F, multipoint control</b>	<b>10</b>
<b>17. PSD Foot F, single-point control</b>	<b>11</b>
<b>18. Spectra ratio, Foot F to specified, multipoint control</b>	<b>11</b>

## FIGURES (Cont'd)

19. Spectra ratio, Foot F to specified, single-point control . . . . .	11
20. Multipoint vs single-point control, acceleration levels at each of the six attachment points . . . . .	11
21. Multipoint control of the low-frequency sine sweep, Foot C . . . . .	12
22. Single-point control of Foot F during low-frequency sine sweep, response of Foot B and C . . . . .	12
23. Multipoint control vs single-point control of the high-frequency sine sweep . . . . .	13

## ABSTRACT

Vibration tests performed at JPL on early *Ranger* spacecraft were made using single-point control of the input vibratory accelerations. The results of these tests clearly showed the inadequacies inherent in this method of control for large structures. Because the fixture required to attach the *Ranger* spacecraft to the shaker could not be made rigid throughout the frequency range of the test, uncontrolled inputs resulted at all the spacecraft mounting points except the point being controlled. A method for controlling each mounting point was required if realistic vibration tests were to be made. A six-channel control system was developed and put into use on *Ranger* Block III spacecraft (*Rangers VII-IX*). The control system operated in two modes: (1) automatic selection and control on the highest acceleration sensed by any one of the six control accelerometers; (2) control on the square root of the sum of the squares of the acceleration sensed by the six control accelerometers. The results obtained from single-point control demonstrate that the spacecraft input is greatly affected by control point selection. That is, an overtest or undertest will occur depending on which point is selected for control. With multipoint control, the input at each mounting point is not controlled perfectly. However, the test requirements are satisfied, and that is not possible with single-point control. Multipoint control also yields a predetermined upper bound that any one mounting point cannot exceed, thus, in effect, holding all the mounting points within a narrower band than could be realized with single-point control.

## I. INTRODUCTION

Test specifications in general require that the input acceleration be controlled at the test specimen's normal attachment point. When an article has several attachment points, a significant question arises as to which point should be chosen for control. Typically, the acceleration at each attachment point varies widely with frequency, and regardless of which attachment point is selected for control, the specification requirements would be compro-

mised since overtesting and undertesting must occur at various frequencies in the test range.

In the case of spacecraft testing, a more sophisticated approach is to control each attachment point independently. Such an approach, which requires the use of a separate shaker system for each attachment point, has gained wide attention in the last few years and has been

applied with satisfactory results. However, it is impractical in many cases in which consideration must be given to cost, equipment size, and output force in relation to the test specification and test article.

This report presents test results of the *Ranger IX* flight-acceptance vibration tests, wherein the six attachment points of the spacecraft were controlled simultaneously with a six-channel multipoint control system designed and built at JPL (Ref. 1). These results are compared with the results of the more traditional method of single-point control.

## II. BACKGROUND OF MULTIPOINT CONTROL AT JPL

Early in the *Ranger* program it became apparent that single-point control of a full spacecraft was unacceptable since excessive acceleration gradients occurred at the spacecraft attachment points. This was primarily caused by the large fixture required for shaker attachment. One of the six spacecraft attachment points could be properly controlled using single-point control, but the acceleration input at the other five attachment points was a function of fixture response; therefore the desired overall spacecraft input was unobtainable.

JPL's first control system was built to control the acceleration input to the *Ranger* spacecraft during structural, proof, and flight-acceptance vibration testing. The system consisted of two accelerometer input channels and furnished an output signal to the servo system which represented the quadratic mean acceleration value sensed by the two-control accelerometers.

$$\text{quadratic mean} = a_c = \sqrt{\frac{a_1^2 + a_2^2}{2}}$$

It follows from the above equation that if either control channel goes to zero, the remaining control channel can only go to 1.41 times the specified level, thereby automatically limiting the level at any control point. The results of the tests performed using the two-channel control system demonstrated that closer adherence to the desired input was obtained, and that further improvement could be realized if all six of the *Ranger* mounting points

Two types of multipoint control are discussed: (1) automatic selection and control of the highest acceleration sensed by any one of the six control accelerometers, and (2) control of the square root of the sum of the squares of the accelerations sensed by the six control accelerometers ("quadratic mean" acceleration).

JPL-developed multipoint control systems have been utilized in vibration testing of hardware and spacecraft systems since 1962. Solar panels, satellite positioning rocket engines, and *Ranger* and *Mariner* spacecraft have been satisfactorily tested using multipoint control.

were controlled by the quadratic mean generated by this relationship:

$$a_c = \sqrt{\frac{E_A^2 + E_B^2 + E_C^2 + E_D^2 + E_E^2 + E_F^2}{6}}$$

mechanized as shown in Fig. 1.

The large bowl-type fixture required for the *Ranger* spacecraft has undesirable dynamic characteristics for vibration testing (Fig. 2). The bowl transfer characteristics are represented by the lower curve in Fig. 3, which is an X-Y recording of the servo control voltage required to hold 5 g rms from 20 to 2000 cps with single-point control. The upper curve is the resultant acceleration sensed by the single control accelerometer mounted at one of the *Ranger* mounting points. From 890 to 2000 cps, the mounting point selected for control is essentially uncontrolled because of fixture resonances in that region. This lack of control is due to the extremely high amplification at the resonances (+40 db), which the servo system is unable to follow.

The lower curve in Fig. 4 is an X-Y recording of the servo control voltage required to hold 5 g rms, quadratic mean acceleration level of six control accelerometers from 100 to 2000 cps. The six accelerometers were mounted at each *Ranger* mounting point. The upper trace shown is the resultant quadratic mean acceleration. The dynamic response of the fixture which caused loss of

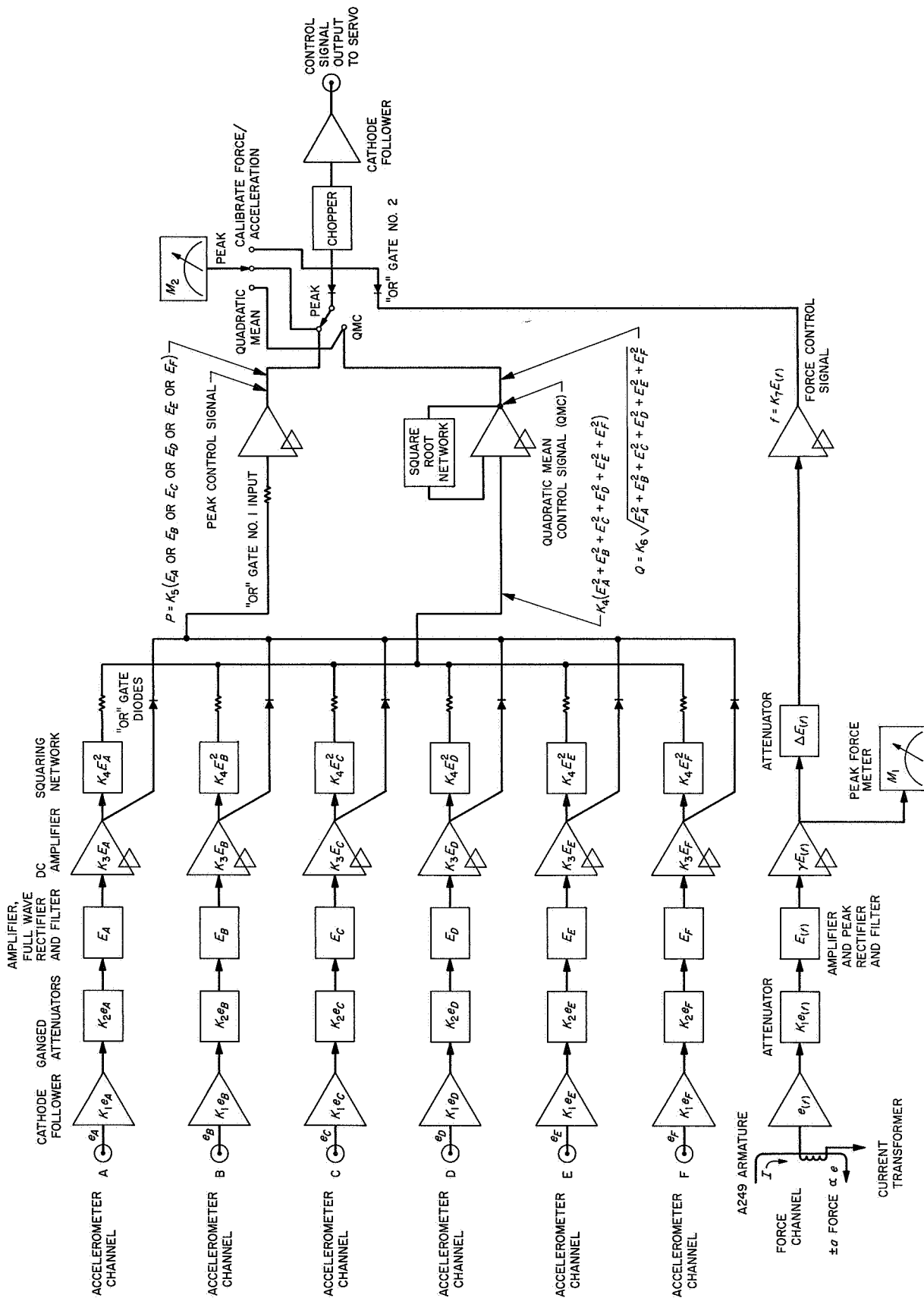
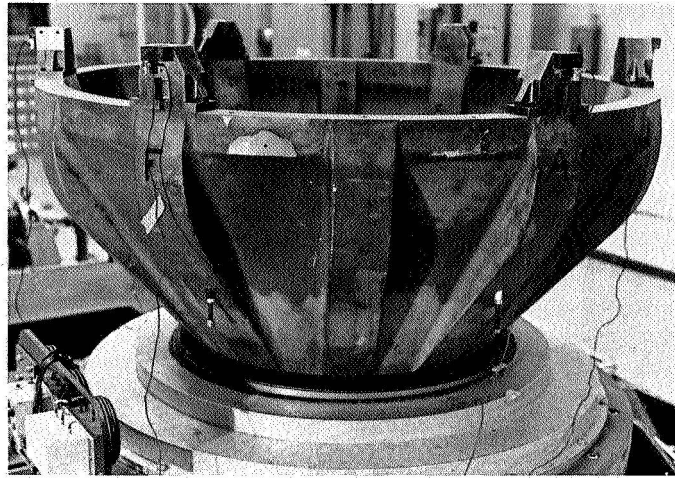
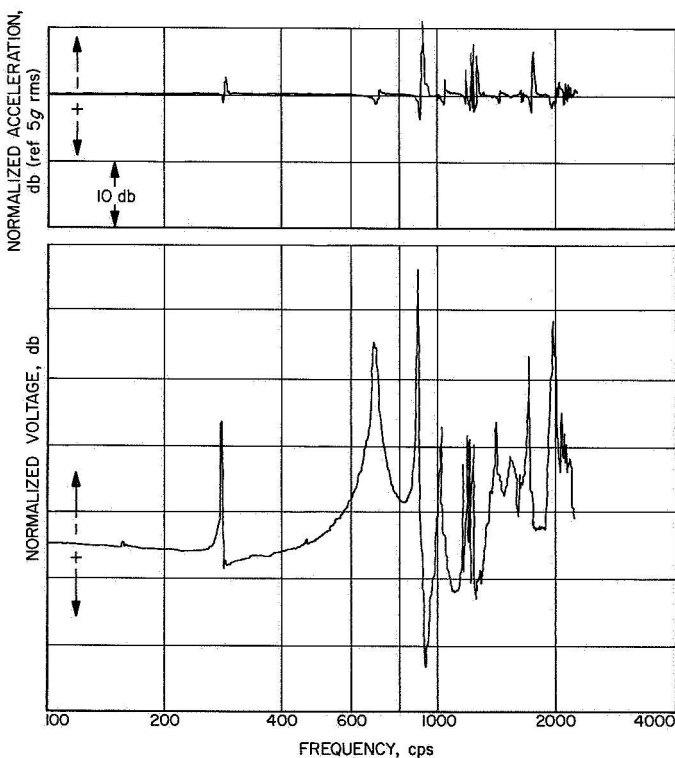


Fig. 1. Functional block diagram of the six-channel multipoint control system



**Fig. 2. Ranger spacecraft Z-axis vibration test fixture**



**Fig. 3. Single-point control equalization requirement and servo-controlled acceleration curves**

control above 890 cps when a single accelerometer was used for control has, in effect, been modified electrically by the use of multiple control points. This apparent modification in fixture response allowed the servo system to hold the quadratic mean acceleration level throughout the frequency range to within  $\pm 2$  db except for a 4-db notch at 525 cps.

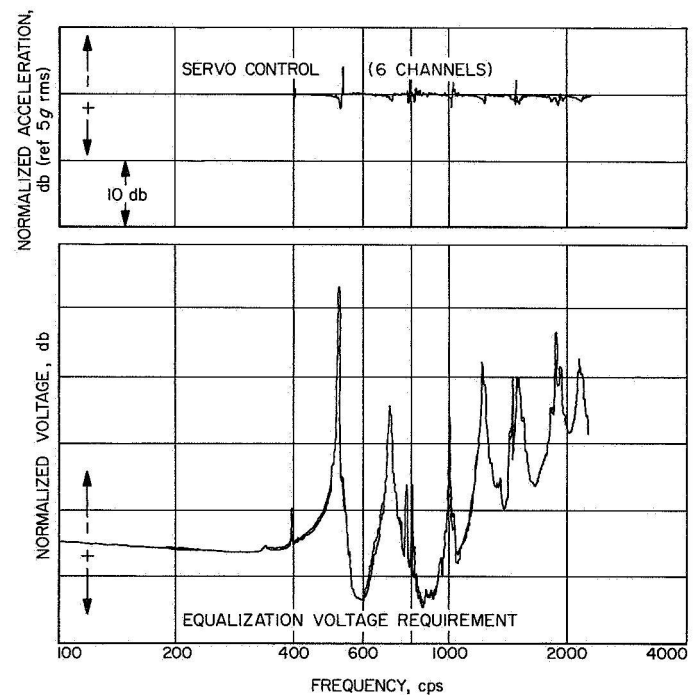


**Fig. 4. Multipoint control equalization requirement and servo-controlled acceleration curves**

From the preceding results, it was clear that multipoint control was superior for testing spacecraft systems. Figure 5 shows a prototype six-channel control system instrument. The left side of the device contains a selector and meter calibrated in terms of force-pounds (driver coil current). The force channel was included to limit the input force to the spacecraft below 100 cps. The limiting value was based on structural considerations associated with the spacecraft adapter.

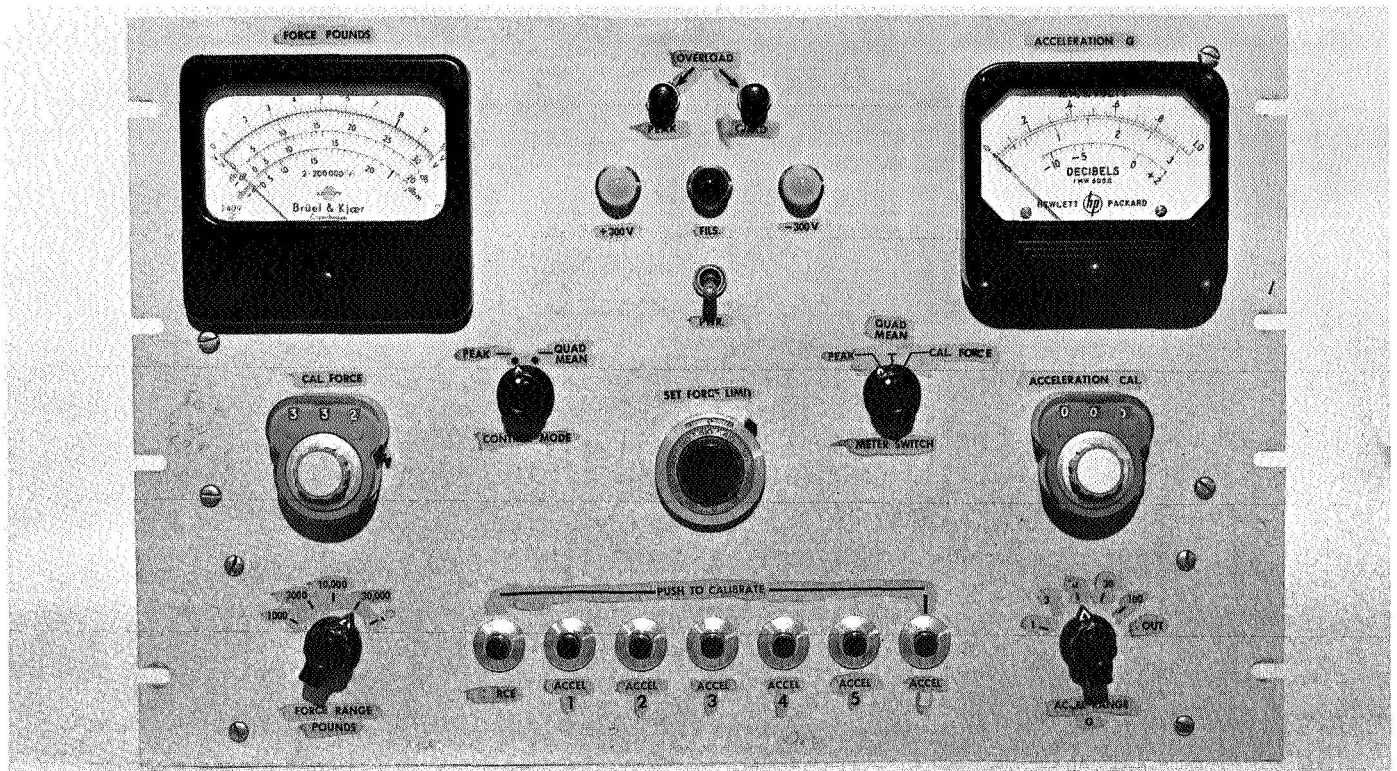


Fig. 5. JPL six-channel control system

### III. EQUALIZATION TECHNIQUES USING MULTIPOINT CONTROL

During the *Ranger* spacecraft testing, vibration system equalization for random noise testing was accomplished with peak/notch equalizers and the shaker system operated open-loop during the random noise test. This method was necessary because in conditioning the six control accelerometer signals the frequency information was lost, thereby making spectrum noise equalization impossible. Consequently, we were faced with the choice of single-point control with spectrum noise equalization or multipoint control and manual sine equalization. Since single-point control had previously proved to be unsatisfactory, we decided on multipoint control.

Following the mounting of the fixture and spacecraft on the shaker, the first step in equalizing the vibration system is to determine the shape of the power amplifier input voltage as a function of frequency required to give a

constant quadratic mean acceleration level obtained from the accelerations sensed by the six control accelerometers.

To obtain a plot of this curve, the system represented in Fig. 6 is used. A sinusoidal vibration sweep is performed from 100 to 2000 cps while the quadratic mean acceleration level is servo-controlled at a constant 0.75 g rms. The X-Y recorder is used to plot the inverse transfer function of the system (equalization requirement curve) on Channel Y2 and to record the input level to the spacecraft on Y1 in order to ascertain that the level is constant. A typical plot is shown in Fig. 7.

The next step, performed with the vibration system off, is to adjust the filter system so that, with a constant signal voltage into the equalization system, the input voltage to the vibration system power amplifier is that voltage

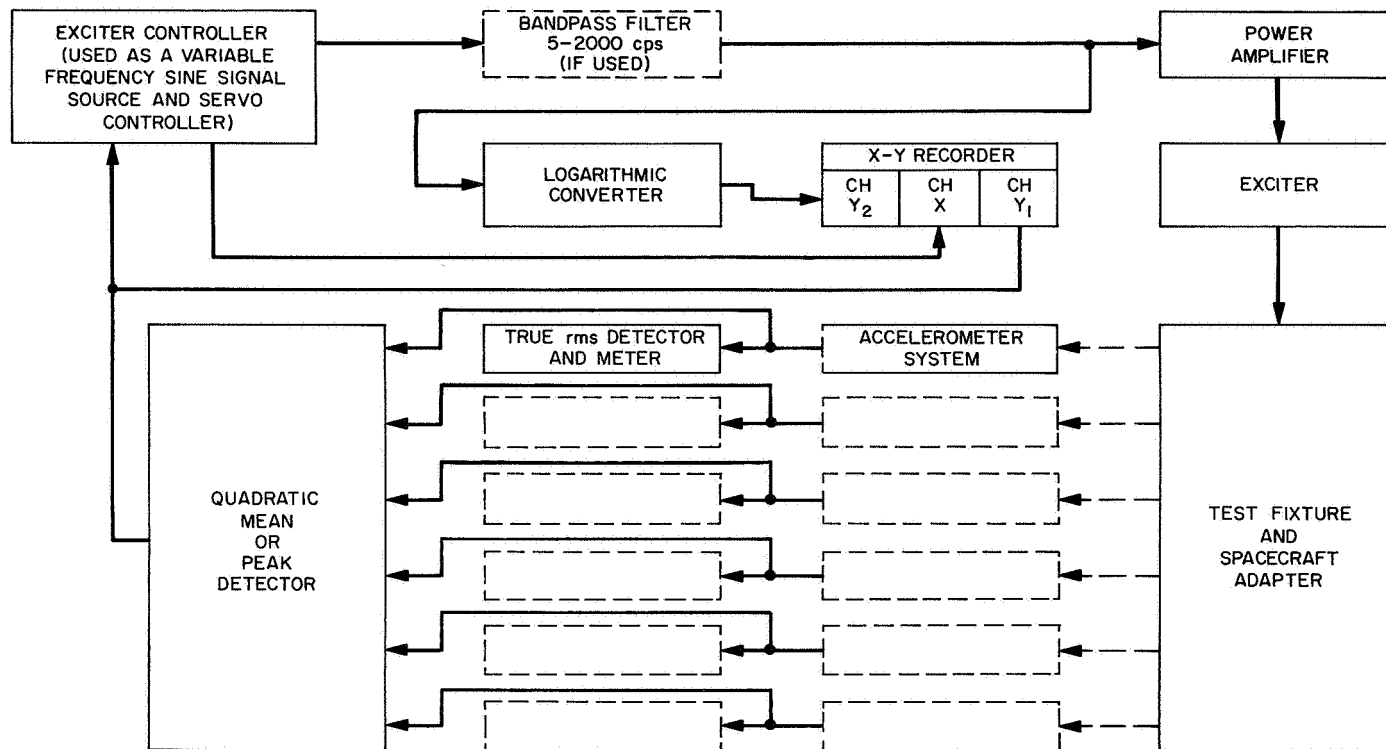


Fig. 6. Functional block diagram for determining equalization requirement curve

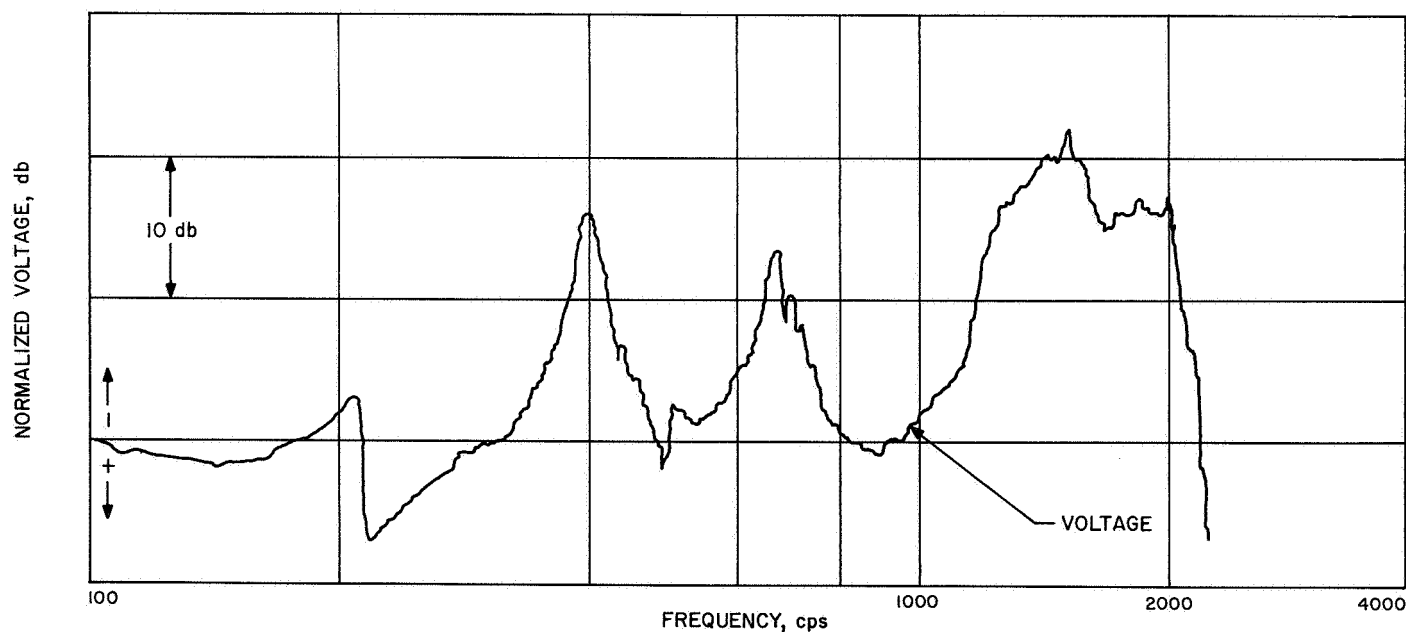


Fig. 7. Equalization requirement curve

required to produce a constant acceleration level at the input to the spacecraft at any frequency within the test range. The proper equalization is indicated when the frequency of the constant-amplitude signal input to the equalization system is varied across the test range and the X-Y recorder pen (Y2) exactly traces the inverse transfer function curve as shown in Fig. 7. The block diagram shown in Fig. 8 represents the system configuration during this step. With this procedure completed, a random noise input signal of a given power spectral density (PSD) will produce approximately the same PSD at the input to the spacecraft.

Verification that the equalization system has been properly adjusted is performed with the vibration system in operation and the system arranged as shown in Fig. 8.

A constant-amplitude sine-wave signal is fed into the equalization system and the frequency varied over the test range. The quadratic mean acceleration level is adjusted to 0.75 g rms and plotted on the X-Y recorder as a function of frequency. If the resultant plot indicates a satisfactory equalization, testing may proceed; otherwise further adjustment of the peak and notch filters must be completed and another verification sweep performed.

The equalization verification plot represented in Fig. 9 is typical of the equalizations achieved by this method. This plot represents the equalization obtained with multi-point control of *Ranger IX* mounted on the bowl fixture shown in Fig. 1. The spacecraft/shaker system was equalized flat within  $\pm 1.5$  db as required by JPL spacecraft test specifications.

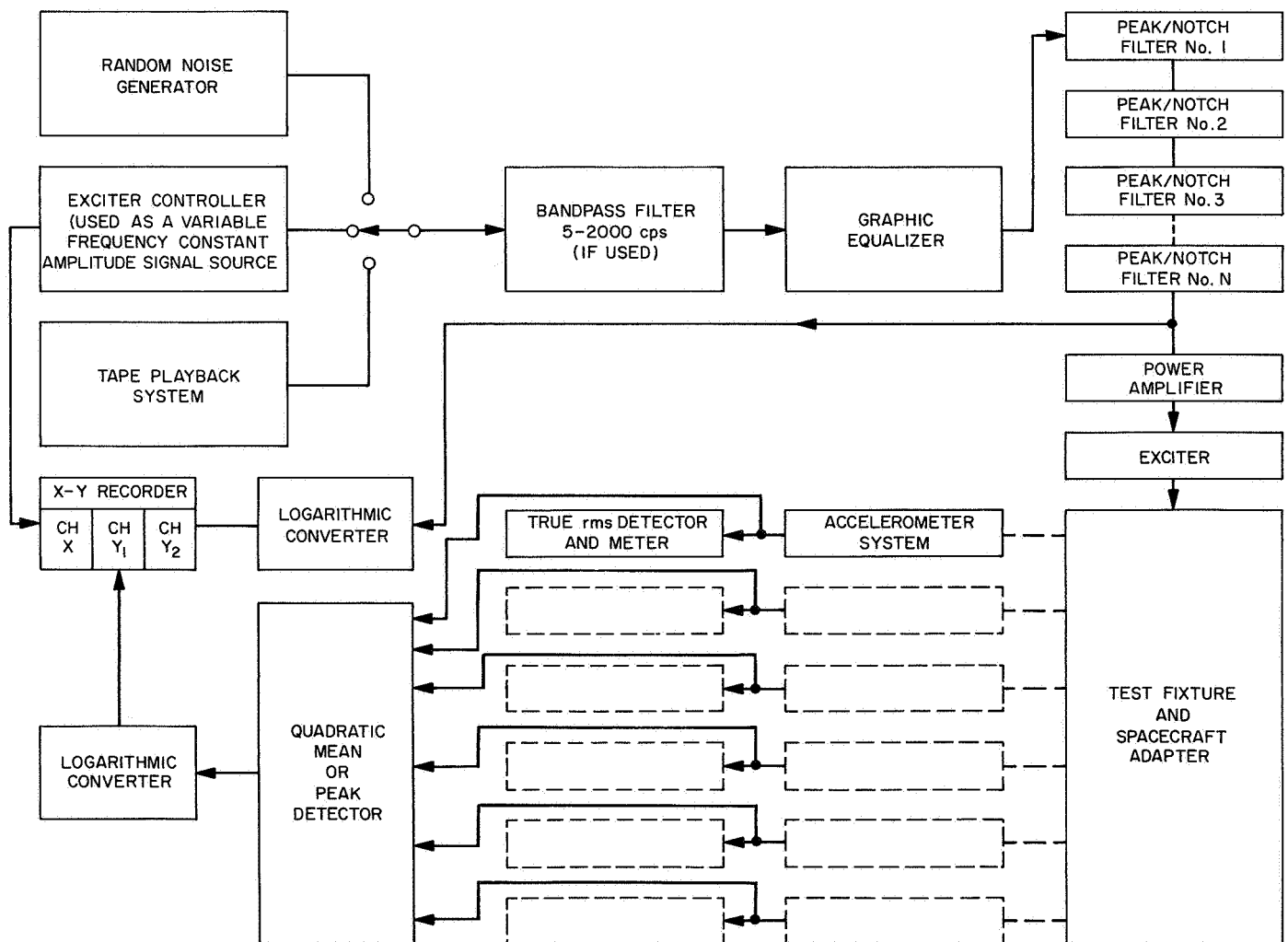


Fig. 8. Functional block diagram for verifying equalization and/or testing

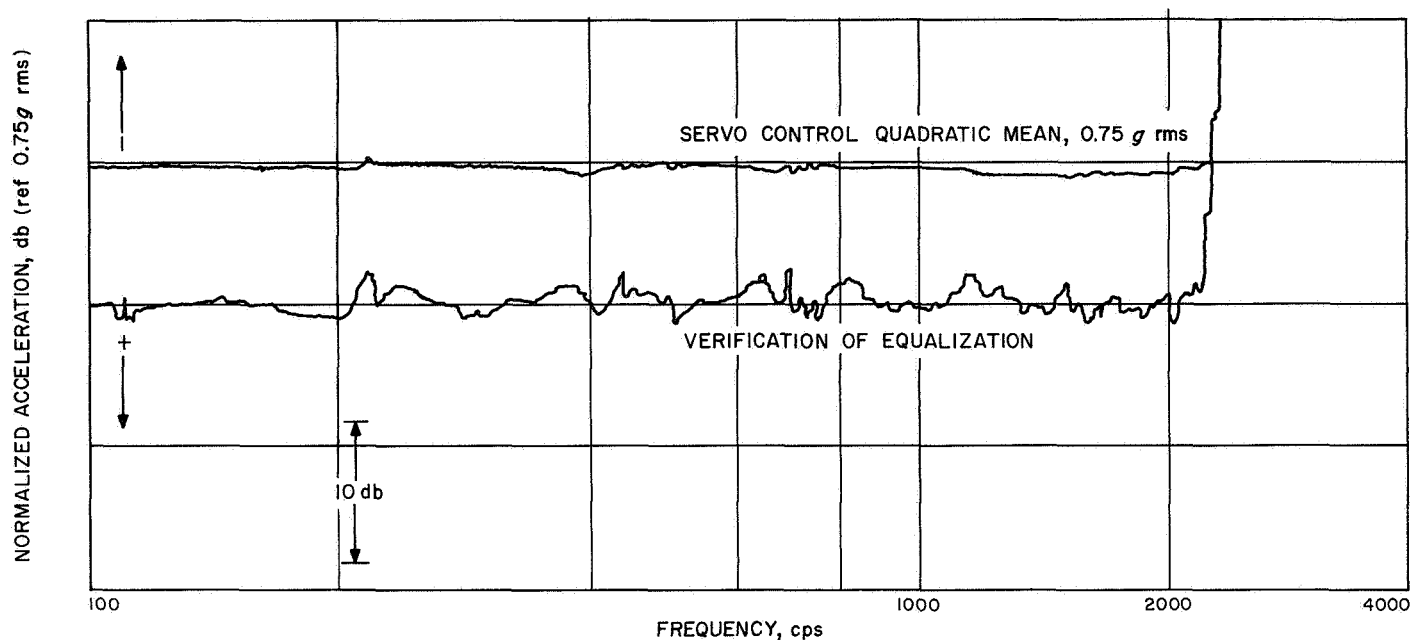


Fig. 9. Equalization verification curve

The sinusoidal equalization method presents certain problems:

1. Since equalization must be performed at low levels, linearity of response must be assumed. If the system response is not linear with varying test levels, error can occur even when the low-level verification indicates proper equalization.
2. Since no monitoring devices other than an overall level meter are available with sinusoidal equalization systems, errors in equalization which might occur from system nonlinearities or component malfunction cannot be detected (or corrected) until a recording of the input acceleration signal can be analyzed.

We reduced the severity of these problems by performing the random noise test at one-half the specified level for an 8-sec period after equalization and by analyzing the individual control accelerometers. Since the system is operated open-loop (no servo control), the degree of system nonlinearity can be approximated by the amount of overburst above the desired one-half level. With this known, an appropriate change is made in the system calibration signal level which precedes the full-level noise burst.

The following results demonstrate that multipoint control with sine equalization was an essential requirement for the *Ranger* spacecraft and resulted in a more realistic test than would have been the case if conventional single-point control had been used.

#### IV. COMPARISON OF MULTIPOINT CONTROL VS SINGLE-POINT CONTROL OF RANGER BLOCK III SPACECRAFT

The control accelerometer readings recorded during the *Ranger* spacecraft vibrations tests were analyzed using analog and digital techniques. Analog was used for sine data and digital for noise data. The sine data were reduced to plots of acceleration vs frequency, noise to power spectral density (PSD), and spectra ratio.

Power spectral density plots of each control point were obtained, as well as the PSD average of the six control points. The PSD average is obtained by taking the arithmetic average within each analysis bandwidth of the six control accelerometers. Spectra ratio equals PSD of point(s)  $n$  divided by PSD specified. Units are in db (where  $\text{db} = 20 \log x_1/x_2$ ).

As previously stated, the multipoint results covered in this paper were obtained during *Ranger* spacecraft vibration testing. However, the single-point results were obtained analytically utilizing an IBM 7094 computer. The test specification PSD (Fig. 10) was ratioed with Foot A (assumed control point). A spectra ratio was thus formed which represented Foot A's deviation from the specification during the actual vibration test. This ratio was then multiplied by the PSD's of Feet A through F obtained during the test, resulting in six modified PSD's which represented the PSD's that would have been obtained had Foot A been used for control. That is to say, the modified PSD's would have resulted if single-point control of Foot A had been used and the system was linear, since the response ratio between any two points on a linear system is a constant. Therefore, the single-

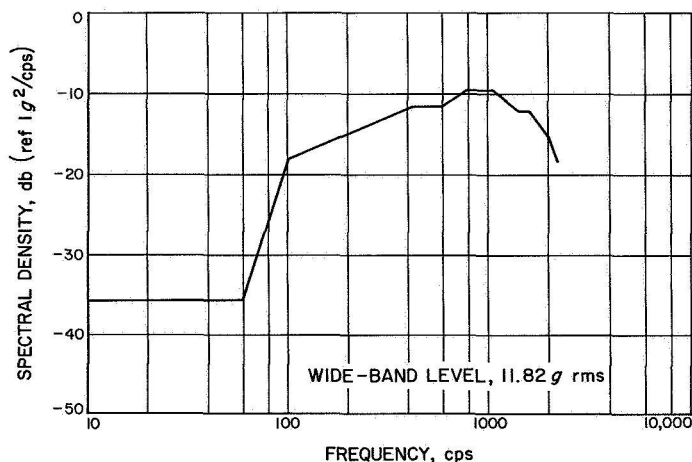


Fig. 10. Test specification power spectral density

point data obtained by this method is valid, and is only compromised if the system is nonlinear. A vibration test setup is shown in Fig. 11.

Figure 12 represents the average PSD of the six control accelerometers. The average PSD of the same accelerometers when only Foot A is controlled is shown in Fig. 13. The specification level is superimposed on each plot for reference. Figures 14 and 15 are of particular interest; they display the spectra ratios corresponding first (in Fig. 14) to multipoint control and second (Fig. 15) to

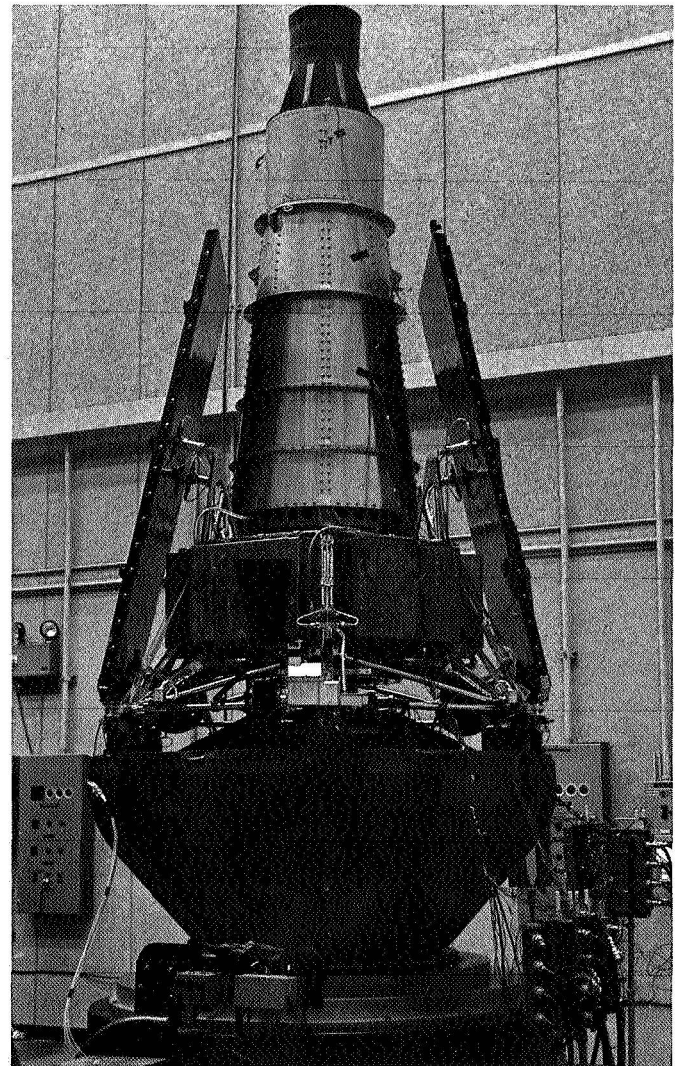


Fig. 11. *Ranger* spacecraft, Z-axis test setup

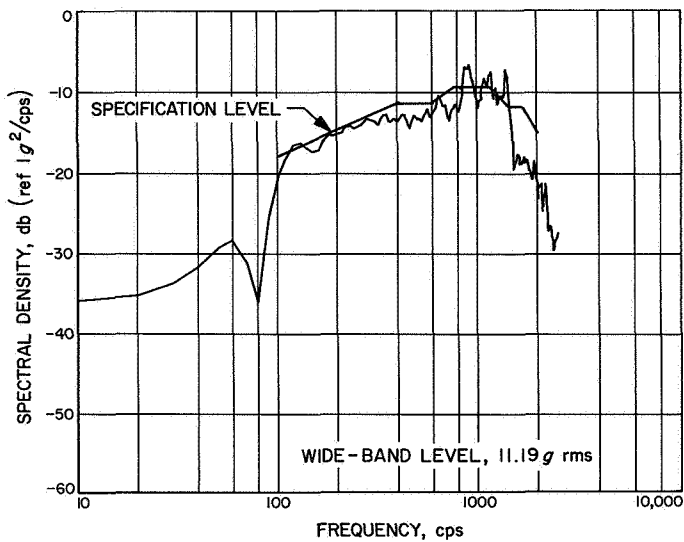


Fig. 12. Average PSD, multipoint control

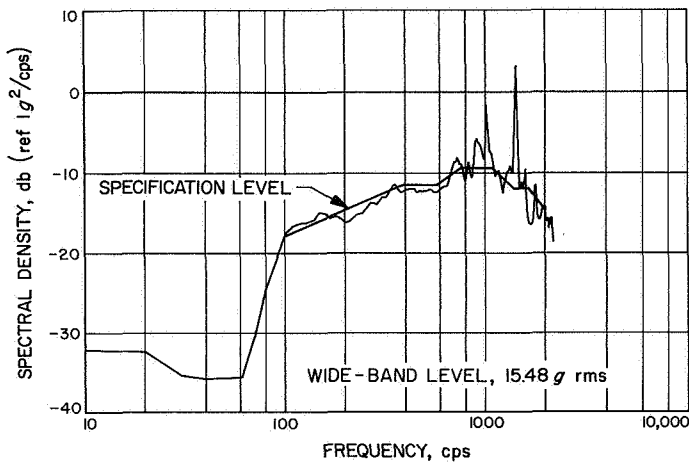


Fig. 13. Average PSD, single-point control

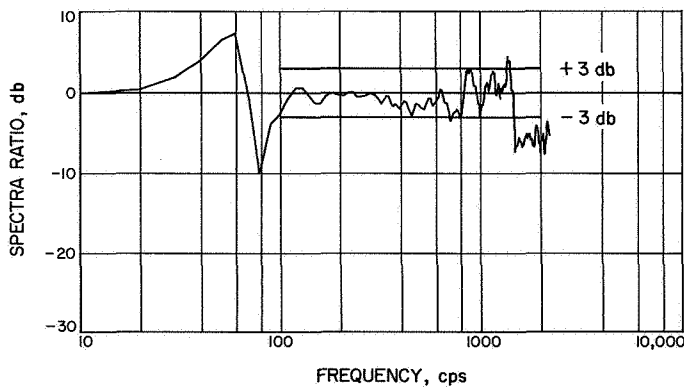


Fig. 14. Spectra ratio, multipoint average ratioed to specification

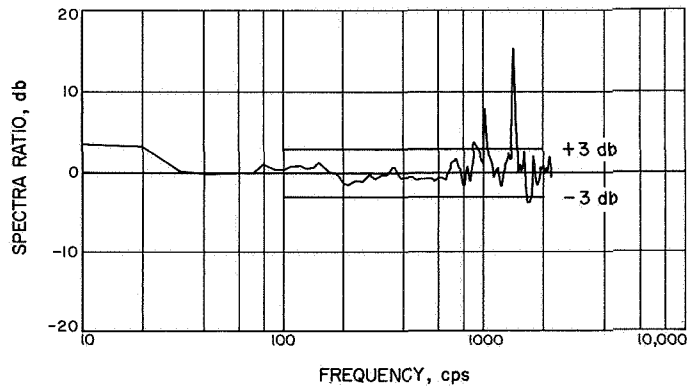


Fig. 15. Spectra ratio, single-point average ratioed to specification

single-point control. If control of all six points had been perfect (that is, if the average PSD produced was identical to the specification PSD), the ratio would be 0 db. For reference purposes,  $\pm 3$ -db lines are plotted on the spectra ratios. The maximum spread with multipoint control is  $+4.5$  to  $-6.5$  db (11 db) and is within  $\pm 3$  db from 100 to approximately 1400 cps. On the other hand, the maximum spread with single-point control is  $+15$  to  $-4$  db (19 db) and goes out of the  $\pm 3$ -db band at approximately 900 cps. Figure 16 represents the PSD at one of the six inputs with multipoint control; the PSD of that same point with single-point control is shown in Fig. 17. The specification level has been superimposed on each PSD. Again, it is clear from inspection of these plots that the PSD resulting from multipoint control more closely resembles the desired level. However, it is difficult to get a clear picture from inspection of these curves

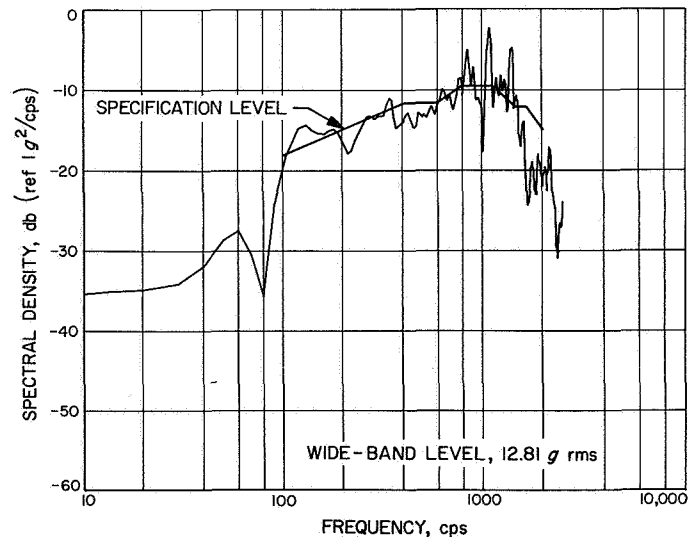


Fig. 16. PSD Foot F, multipoint control

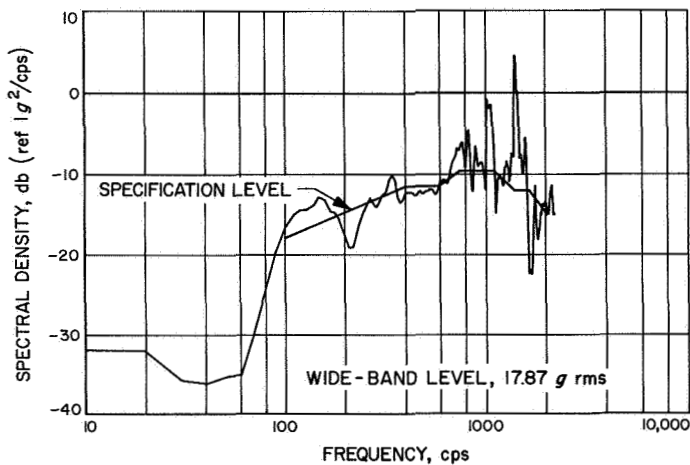


Fig. 17. PSD Foot F, single-point control

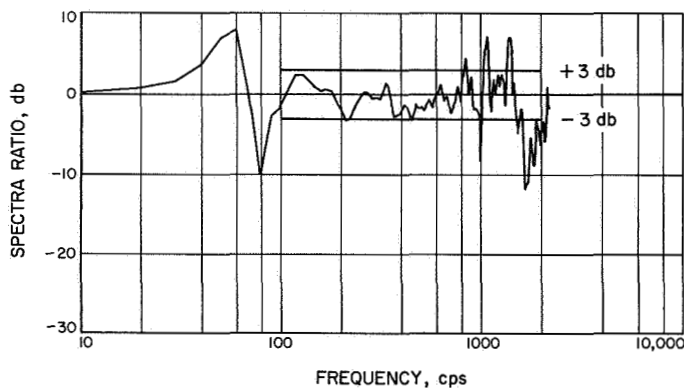


Fig. 18. Spectra ratio, Foot F to specified, multipoint control

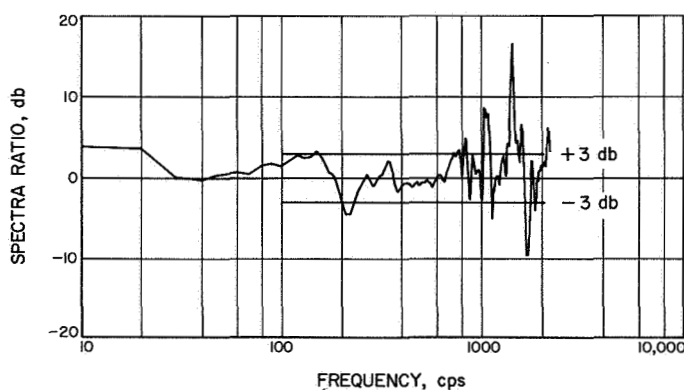


Fig. 19. Spectra ratio, Foot F to specified, single-point control

alone. Figures 18 and 19 present the the spectra ratios—the PSD resulting from multipoint control ratioed to the specification (Fig. 18) vs the PSD resulting from single-point control ratioed to the specification (Fig. 19). Again,

if all inputs were identical, the ratio would be 0 db. The maximum spread shown for multipoint control (Fig. 18) is +7 to -11.5 db (18.5 db) and is within the  $\pm 3$ -db band up to approximately 1400 cps, with the exception of two peaks (+4 and +7 db) and one notch (-8 db). The maximum variation for the single-point plot (Fig. 19) is +17 to -10 db (27 db), going out of the  $\pm 3$ -db band at 225 cps.

It should be noted from the results presented that multipoint control yields a predetermined upper bound; this is not the case with single-point control. The upper bound is determined by

$$a_{max} = x\sqrt{n}$$

where

$a_{max}$  = maximum deviation of any accelerometer from specification level

$n$  = specified level

$x$  = number of control points

Figure 20 is a plot of the wide-band rms acceleration levels measured at each attachment point. The measured level is plotted as the ordinate; the attachment points (1-6) are plotted as the abscissa. The specification level

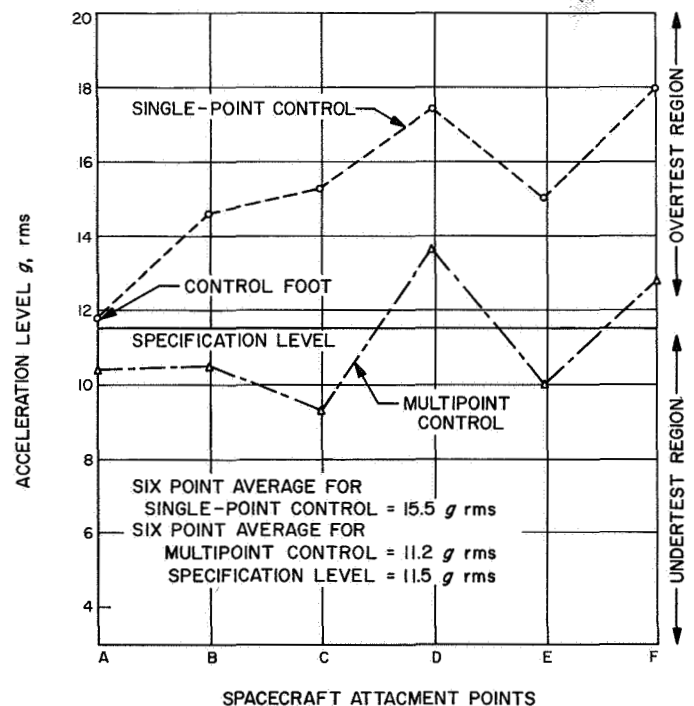


Fig. 20. Multipoint vs single-point control, acceleration levels at each of the six attachment points

of 11.5 g rms is plotted as a straight line, since ideally all the attachment points should be identical. From these curves it is clear that with single-point control of Foot A all other attachment points would be high, resulting in a quadratic mean acceleration input level of 15.5 g rms and an overtest. With multipoint control, the quadratic mean acceleration input level was 11.2 g rms, well within the specified tolerance of  $\pm 10\%$ . The amount of overtest resulting from control of Foot A would not have occurred if some other attachment point had been selected for control. In fact, if Foot F had been chosen, an undertest would have resulted. Of particular interest here is the fact that the test performed with single-point control is a function of the point that is used for control and not the control system as desired. In other words, the input to the spacecraft is more dependent on the dynamic response of the fixture when single-point control is used.

There are two sinusoidal testing requirements for *Ranger* spacecraft: low-frequency sine sweep (20–130 cps) and high-frequency sine sweep (130–2000 cps). Structural considerations dictate that, for flight acceptance testing,

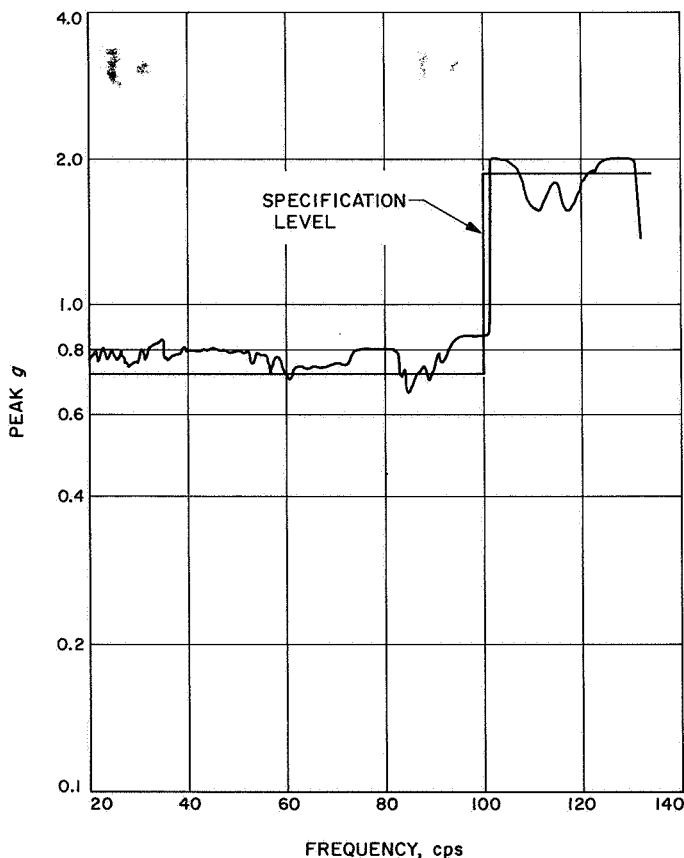


Fig. 21. Multipoint control of the low-frequency sine sweep, Foot C

no attachment point shall exceed a given level during the low-frequency test.

Figure 21 represents the acceleration level of Foot C during the low-frequency test, wherein the multipoint control system was operated in the peak select mode (i.e., automatically selecting the highest acceleration level sensed by any one of the six control accelerometers and controlling that point at a given level). As shown in Fig. 21, Foot C never exceeded the preset level and controlled during four distinct portions of the sweep, approximately 73 to 83 cps. In contrast, Fig. 22 represents the acceleration levels sensed at Feet B and C, with Foot F controlled perfectly. It is immediately apparent from these curves that, with single-point control, the test requirement cannot be met, since Feet B and C both exceed the control level and an overtest results.

For the high-frequency test, it is desired to control the quadratic mean acceleration input level. Figure 23 represents the arithmetic average of the six control accel-

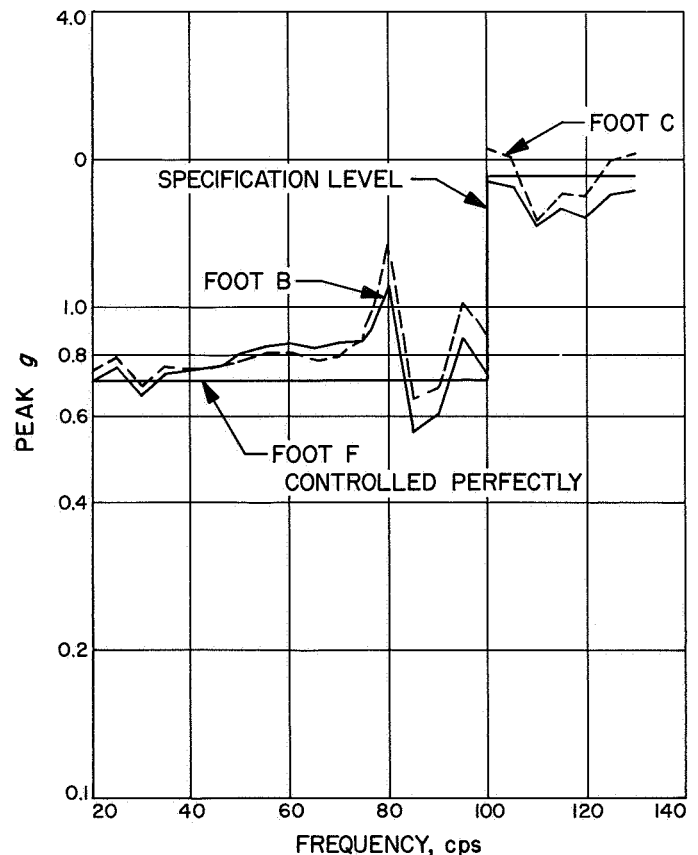
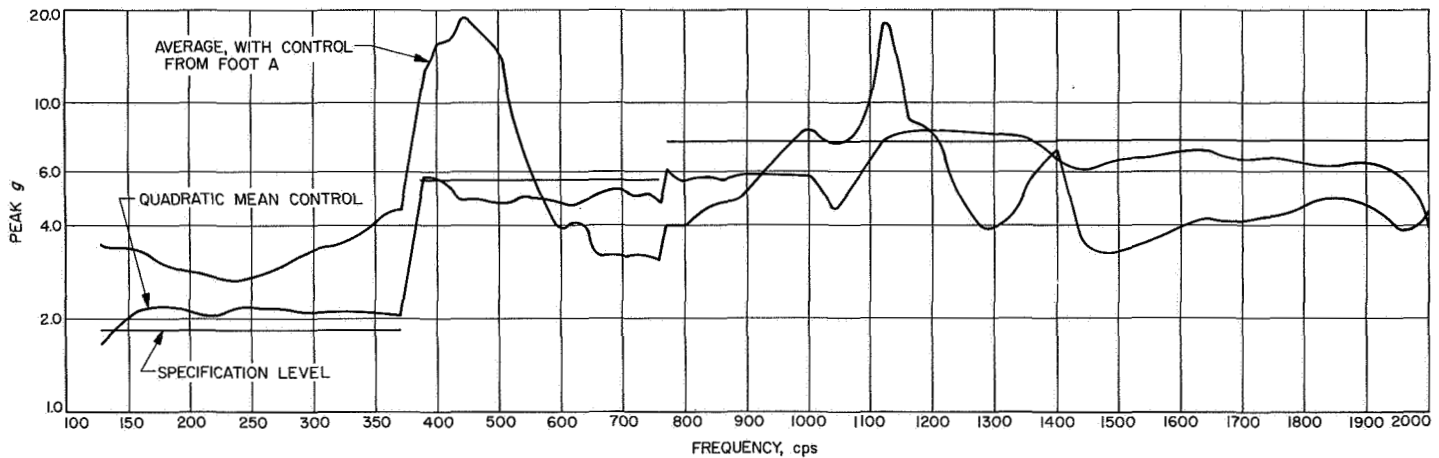


Fig. 22. Single-point control of Foot F during low-frequency sine sweep, response of Foot B and C



**Fig. 23. Multipoint control vs single-point control of the high-frequency sine sweep**

erometers when multipoint control (quadratic mean) was used and the arithmetic average of the same accelerometers when Foot A was controlled perfectly. The specification level is also plotted for reference. Once again, it is clear that the six-accelerometer average variation asso-

ciated with single-point is, in general, greater than that encountered with multipoint control. To reiterate, these variations will change as the control point is changed, with the response of the fixture playing a dominant role in affecting the spacecraft input.

## V. CONCLUSIONS

It is apparent that the use of multipoint control for *Ranger* vibration tests was a definite step forward in the improvement of vibration simulation at JPL. However, this is not to say that the type of multipoint control used is a solution for all the control problems facing the environmental engineer today. As was pointed out and demonstrated here, many compromises still must be made if multipoint control is used. For example, automatic noise equalization systems cannot be employed. What must be done now is to develop more versatile multipoint control systems which will allow the use of automatic systems. In the case of the JPL system, increased dynamic range is needed with faster response and correspondingly greater stability. The controversy

over how best to control the vibration environment specified, instead of decreasing, will increase with the advent of new control systems, since more and more problems are arising as test structures increase in size.

At JPL, we are presently working on new control systems to solve some of the current problems (Ref. 2). For example, under study is a six-channel peak selection device which is solid state and compatible with current automatic equalization systems. Another interesting control concept being investigated relates to the control of the cross-correlation function during noise testing. The results of these studies will be reported when available.

## REFERENCES

1. R. Woodbury (Jet Propulsion Laboratory), unpublished work.
2. P. Chapman, "Six Channel Automatic Accelerometer Selector," *Space Program Summary 37-35, Volume VI*, Jet Propulsion Laboratory, Pasadena, Calif., October 1965.

## ACKNOWLEDGMENT

The author wishes to thank A. Bowman, J. Drugan, M. Trummel, R. Goggia, and R. Woodbury for assistance in various phases of the experimental work reported herein.